EPJ Web of Conferences **85**, 02017 (2015)
DOI: 10.1051/epjconf/ 20158502017

Phenomenology of COMPASS data

Multiplicities and Phenomenology - Part II

M. Anselmino[1,2,a], M. Boglione[1,2,b], J.O. Gonzalez H.[2,c], S. Melis[1,d], and A. Prokudin[3,e]

[1] *Dipartimento di Fisica Teorica, Università di Torino, Via P. Giuria 1, I-10125 Torino, Italy*
[2] *INFN, Sezione di Torino, Via P. Giuria 1, I-10125 Torino, Italy*
[3] *Jefferson Laboratory, 12000 Jefferson Avenue, Newport News, VA 23606, USA*

Abstract. We present some of the main features of the multidimensional COMPASS multiplicities, via our analysis using the simple Gaussian model. We briefly discuss these results in connection with azimuthal asymmetries.

1 Introduction

Multidimensional Semi-Inclusive Deep Inelastic Scattering (SIDIS) data recently released by the COMPASS collaboration [1], present a unique opportunity to study x, z and Q^2 dependences of the unpolarized Transverse Momentum Dependent Distribution and Fragmentation functions (TMDs). Of particular interest is the study of the Q^2 dependence of TMDs, in the context of TMD-evolution, which in principle may be observed in these multiplicities. However, some aspects of the data make it non-trivial to draw any sensible conclusion when using a TMD-evolution scheme. For instance, the kinematics of the data, which include regions were factorization may not necessarily hold, the short range of Q^2 ($1.11\ \text{GeV}^2 - 7.57\ \text{GeV}^2$), which might make it difficult to observe Q^2-evolution, just to mention a few. These features are not unique to the COMPASS data set, neither do these complications arise solely from the nature of the data, but also from the flexibility introduced in any current formalism of TMD evolution, via the prescription used to avoid the Landau pole in b-space and the non-perturbative piece of the TMDs which is model-dependent.

If one is to understand what aspects of an analysis using full TMD-evolution arise from QCD and which ones are just the result of a flexible enough parametrization, it is necessary to have a control analysis or a “benchmark". We performed such an analysis for the COMPASS multiplicities, which serves as the first step towards the extraction of the universal unpolarized TMDs. The present work is a summary of our analysis, already published in Ref. [2]. We also show some preliminary results from our ongoing analysis of COMPASS azimuthal asymmetries [3].

[a] e-mail: anselmino@to.infn.it
[b] e-mail: boglione@to.infn.it
[c] e-mail: joseosvaldo.gonzalez@to.infn.it
[d] e-mail: melis@to.infn.it
[e] e-mail: prokudin@jlab.gov

2 A first Glance at the Data

Before presenting the results of our analysis, in this section we will describe some of the features of the COMPASS multiplicities. These observations are important when constructing a model for the unpolarized TMDs.

The most noticeable feature of the COMPASS data set is the strong variation of its normalisation in the $x\,Q^2$ plane. To illustrate the trend of the data, Figure 1 shows a selection of multiplicities, for which interpolation curves have been drawn in the following way: first, interpolating the data in the 5 bottom panels, for two bins of z (red and green), then using each of these curves in the upper panel that best matches the value of y of the interpolated data. For instance, all of the red curves in the three leftmost panels are the same. This simple exercise, shows that for the same value of z, the data on panels along the ”diagonal“ in the $x\,Q^2$-plane seem to have not only very similar width, but also roughly the same normalisation. This signals an unexpected dependence on y of the COMPASS multiplicities. Furthermore, the blue lines in Figure 1 show that the normalisation can be roughly approximated by a straight line. Note that trend is a feature of the data alone, as no use of any model has been made for this very simple exercise. This observation must be taken into account when using these multiplicities in any attempt to extract the Unpolarized TMDs. It must be noted that such a behaviour is not likely to be connected to TMD-evolution, which effects are expected to be much smaller in this kinematical range.

3 Formalism

The unpolarised $\ell + p \to \ell' h X$ SIDIS cross section in the TMD factorisation scheme, at order $(k_\perp/Q)$ and α_s^0, in the

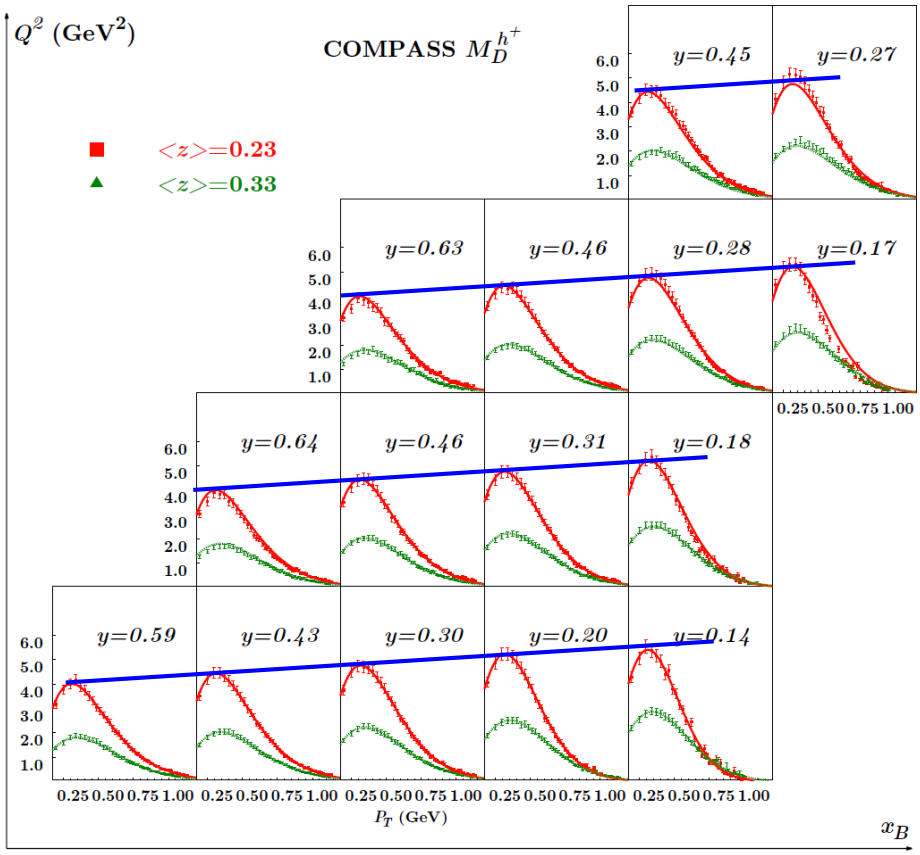

Figure 1. A selection of the COMPASS multiplicities data. Solid lines are interpolation curves for the 5 panels at the bottom. The same interpolation lines have been used for top panels, matching values of z and y (see text). Blue lines are all parallel to each other. This illustrates the roughly linear dependence on y of the normalisation of the multiplicities.

kinematical region where $P_T \simeq k_\perp \ll Q$, reads [4, 5]:

$$\frac{d\sigma^{\ell+p\to\ell' hX}}{dx_B\, dQ^2\, dz_h\, dP_T^2} = \frac{2\pi^2\alpha^2}{(x_B s)^2}\,\frac{\left[1+(1-y)^2\right]}{y^2}\,F_{UU} \qquad (1)$$

$$F_{UU} \equiv \sum_q e_q^2 \int d^2\boldsymbol{k}_\perp \; f_{q/p}(x,k_\perp)\, D_{h/q}(z,p_\perp) \qquad (2)$$

In the $\gamma^* - p$ c.m. frame the measured transverse momentum, $\boldsymbol{P}_T$, of the final hadron is given at order $k_\perp/Q$ by $\boldsymbol{P}_T = z_h\,\boldsymbol{k}_\perp + \boldsymbol{p}_\perp$. The exact relations can be found in Ref. [6]. Furthermore, we assume for the $k_\perp$ and $p_\perp$ dependences a Gaussian form, factorized from other kinematical variables,

$$f_{q/p}(x,k_\perp) \;=\; f_{q/p}(x)\,\frac{e^{-k_\perp^2/\langle k_\perp^2\rangle}}{\pi\langle k_\perp^2\rangle}\,, \qquad (3a)$$

$$D_{h/q}(z,p_\perp) \;=\; D_{h/q}(z)\,\frac{e^{-p_\perp^2/\langle p_\perp^2\rangle}}{\pi\langle p_\perp^2\rangle}\,. \qquad (3b)$$

The integrated parton distribution functions (PDFs) and fragmentation functions (FFs) , $f_{q/p}(x)$ and $D_{h/q}(z)$, can be taken from the available fits of the world data: in this analysis we used the CTEQ6L set for the PDFs [7] and the DSS set for the fragmentation functions [8]. In the simple Gaussian parameterisation, supported by a number of experimental evidences [9] as well as by dedicated lattice simulations [10], by inserting Eqs. (3) into Eq. (2), one obtains

$$F_{UU} = \sum_q e_q^2\, f_{q/p}(x_B)\, D_{h/q}(z_h)\,\frac{e^{-P_T^2/\langle P_T^2\rangle}}{\pi\langle P_T^2\rangle}\,, \qquad (4)$$

where $\langle P_T^2\rangle$ is given by

$$\langle P_T^2\rangle = \langle p_\perp^2\rangle + z_h^2\,\langle k_\perp^2\rangle\,. \qquad (5)$$

For the multiplicities, defined as $M_n^h \equiv \sigma^{SIDIS}/\sigma^{DIS}$ (see reference [2] for further details), one gets

$$\frac{1}{2P_T} M_n^h(x_B,Q^2,z_h,P_T) = \frac{\pi\,\sum_q e_q^2\, f_{q/p}(x_B)\, D_{h/q}(z_h)}{\sum_q e_q^2\, f_{q/p}(x_B)}\,\frac{e^{-P_T^2/\langle P_T^2\rangle}}{\pi\langle P_T^2\rangle}\,, \qquad (6)$$

with $\langle P_T^2\rangle$ given in Eq. (5). Notice that $\langle k_\perp^2\rangle$ and $\langle p_\perp^2\rangle$ are the free parameters of our fit.

4 Results on multiplicities

In this section we show the results from two different fits on the COMPASS SIDIS multiplicities of Ref. [1]. In both fits, we used the model of Eqs. (3). Only in the second fit, we used an extra normalisation factor for the multiplicities,

to account for the trend of the data explained in section 2. Such normalisation was parameterised as

$$N_y = N_1 + y\,N_2, \tag{7}$$

which introduces two additional parameters, for the entire subset of data considered in the fit. Results are shown in table 1 and Figure 2. From these two fits, one can readily see that the value of χ^2 is dramatically reduced by introducing the normalisation of Eq. (7), while the values of the widths for the TMDs remain essentially the same. This is expected from the observations made in section 2. Notice that the still sizeable value of χ^2_{dof} receives a large contribution from those bins with low values of y, enclosed in red boxes in Fig. 2. In fact, except for those bins, the simple Gaussian model of Eq. (3) makes a rather remarkable job in reproducing the COMPASS data. Following this analysis, one can see that any effect introduced by Q^2-evolution must be very subtle, in the considered kinematics.

5 Azimuthal Asymmetries and Parameter Interpretation

The results of our analysis are relevant not only when looking at the multiplicities, but also regarding the data on $\langle cos(\phi)\rangle$ and $\langle cos(2\phi)\rangle$ asymmetries of [11]. These asymmetries in principle contain information about the Boer-Mulders and Collins functions. We are currently finalizing the analysis of the COMPASS azimuthal asymmetries, which we will submit for publication in the near future. For the purposes of this discussion, we only want to mention a few key points concerning the parameter interpretation. We then focus only on $\langle cos(\phi)\rangle$ which up to $O(k_\perp/Q)$ receives two contributions

$$\langle cos(\phi)\rangle \propto \frac{\left(F_{UU}^{\cos\phi_h}\right)_{Cahn}}{F_{UU}} + \frac{\left(F_{UU}^{\cos\phi_h}\right)_{BM}}{F_{UU}}, \tag{8}$$

where $(F_{UU}^{\cos\phi_h})_{Cahn}$ depends only on the unpolarized TMDs and $(F_{UU}^{\cos\phi_h})_{BM}$ on both the Boer-Mulders and the Collins functions. F_{UU} is given in Eq. (2). Notice that the Cahn and Boer-Mulders effects in $\langle cos(\phi)\rangle$ cannot be disentangled. It might be tempting to use the TMDs extracted from the analysis in the multiplicities, in order to calculate the Cahn contribution to $\langle cos(\phi)\rangle$, and simply attempt to learn about the Boer-Mulders effect. However, through Eq. (5), one can see that from an analysis on the multiplicities alone, one can only get information about $\left\langle P_T^2\right\rangle = \left\langle p_\perp^2\right\rangle + z_h^2\left\langle p_\perp^2\right\rangle$, and not directly about $\left\langle k_\perp^2\right\rangle$ and $\left\langle p_\perp^2\right\rangle$. It is then a very delicate matter to interpret the parameters of the model. To illustrate this point, let us consider the case in which $\left\langle p_\perp^2\right\rangle$ is z-dependent. To make the argument clearer, we chose the specific functional form

$$\left\langle p_\perp^2\right\rangle = A + z^2\,B. \tag{9}$$

In this case, $\left\langle P_T^2\right\rangle$ can be written as

$$\left\langle P_T^2\right\rangle \to A + z^2\left(\left\langle k_\perp^2\right\rangle + B\right). \tag{10}$$

Looking at Eqs. (5) and (10), and focusing on the term quadratic in z, one would reach two different conclusions about the value of $\left\langle k_\perp^2\right\rangle$. So one cannot really disentangle $\left\langle p_\perp^2\right\rangle$ and $\left\langle k_\perp^2\right\rangle$ without additional information, such as that contained in $\langle cos(\phi)\rangle$. To see why this asymmetry can help in separating $\left\langle p_\perp^2\right\rangle$ from $\left\langle k_\perp^2\right\rangle$, one can focus on the Gaussian model, in which

$$\frac{\left(F_{UU}^{\cos\phi_h}\right)_{Cahn}}{F_{UU}} \propto \frac{\left\langle k_\perp^2\right\rangle}{\left\langle P_T^2\right\rangle}. \tag{11}$$

So the same quantities $\left\langle k_\perp^2\right\rangle$ and $\left\langle p_\perp^2\right\rangle$ appear, but in a configuration different from that of the multiplicities.

Finally, for completeness, we show here preliminary results of a simultaneous fit of the COMPASS data on multiplicities and $\langle cos(\phi)\rangle$, using the parametric form of Eq. (10). In this fit, we have only used the Cahn effect to calculate $\langle cos(\phi)\rangle$. We show in Fig. 3 the results for $\langle cos(\phi)\rangle$. For the multiplicities one gets the same as discussed previously, in Fig 2. The kinematical cuts used in this fits are the same as those shown in Table 1. It must be mentioned that without additional flexibility, introduced through to some scheme like that of Eq. (10), one cannot describe both multiplicities and $\langle cos(\phi)\rangle$ simultaneously. In an forthcoming publication, we will discuss these issues in detail.

References

[1] C. Adolph et al. (COMPASS), *Eur. Phys. J.* **C73** (2531) 2013

[2] M. Anselmino, M. Boglione , J.O. Gonzalez H. , S. Melis, A. Prokudin, *JHEP* **1404** (005) 2014

[3] M. Anselmino, V. Barone, M. Boglione , J.O. Gonzalez H. , S. Melis, (In preparation)

[4] A. Bacchetta, M. Diehl, K. Goeke, A. Metz, P. J. Mulders, et al., *JHEP* **0702** (093) 2007

[5] M. Anselmino, M. Boglione, U. D'Alesio, S. Melis, F. Murgia, et al., *Phys. Rev.* **D83** (114019) 2011

[6] M. Anselmino, M. Boglione, U. D'Alesio, A. Kotzinian, F. Murgia, A. Prokudin, *Phys. Lett.* **D71** (074006) 2005

[7] J. Pumplin, D. Stump, J. Huston, H. Lai, P. M. Nadolsky, et al., *JHEP* **0207** (012) 2002 [hep-ph/0201195]

[8] D.de Florian, R.Sassot, and M.Stratmann., *Phys. Rev.* **D75** (114010) 2007

[9] P Schweitzer, T Teckentrup, A Metz., *Phys. Rev.* **D81** (094019) 2010

[10] B. U. Musch et al., *PoS* **LAT2007** (155) 2007

[11] Adolph, C. et al. (COMPASS), *Nucl.Phys.* **B886** (1046-1077) 2014

Table 1. χ^2 values of our best fits, following Eqs. (2-6), of the experimental COMPASS measurements of the SIDIS multiplicities $M_n^h(x_B, Q^2, z_h, P_T)$ for h^+ and h^- production, off a deuteron target. We show the total $\chi^2_{\rm dof}$ and, separately, the $\chi^2_{\rm dof}$ for h^+ and h^- data. CTEQ6 PDFs and DSS FFs are used. Notice that the errors quoted for the parameters are statistical errors only, and correspond to a 5% variation over the total minimum χ^2. The two lowest rows of numerical results are obtained allowing for a y-dependent extra normalisation factor, Eq. (7).

COMPASS

Cuts	$\chi^2_{\rm dof}$	n. points	$[\chi^2_{\rm point}]^{h^+}$	$[\chi^2_{\rm point}]^{h^-}$	Parameters
$Q^2 > 1.69$ GeV^2 $0.2 < P_T < 0.9$ GeV $z < 0.6$	8.54	5385	8.94	8.15	$\langle k_\perp^2 \rangle = 0.61 \pm 0.20$ GeV^2 $\langle p_\perp^2 \rangle = 0.19 \pm 0.02$ GeV^2
$Q^2 > 1.69$ GeV^2 $0.2 < P_T < 0.9$ GeV $z < 0.6$ $N_y = N_1 + y\,N_2$	3.42	5385	3.25	3.60	$\langle k_\perp^2 \rangle = 0.60 \pm 0.14$ GeV^2 $\langle p_\perp^2 \rangle = 0.20 \pm 0.02$ GeV^2 $N_1 = 1.06 \pm 0.06$ $N_2 = -0.43 \pm 0.14$

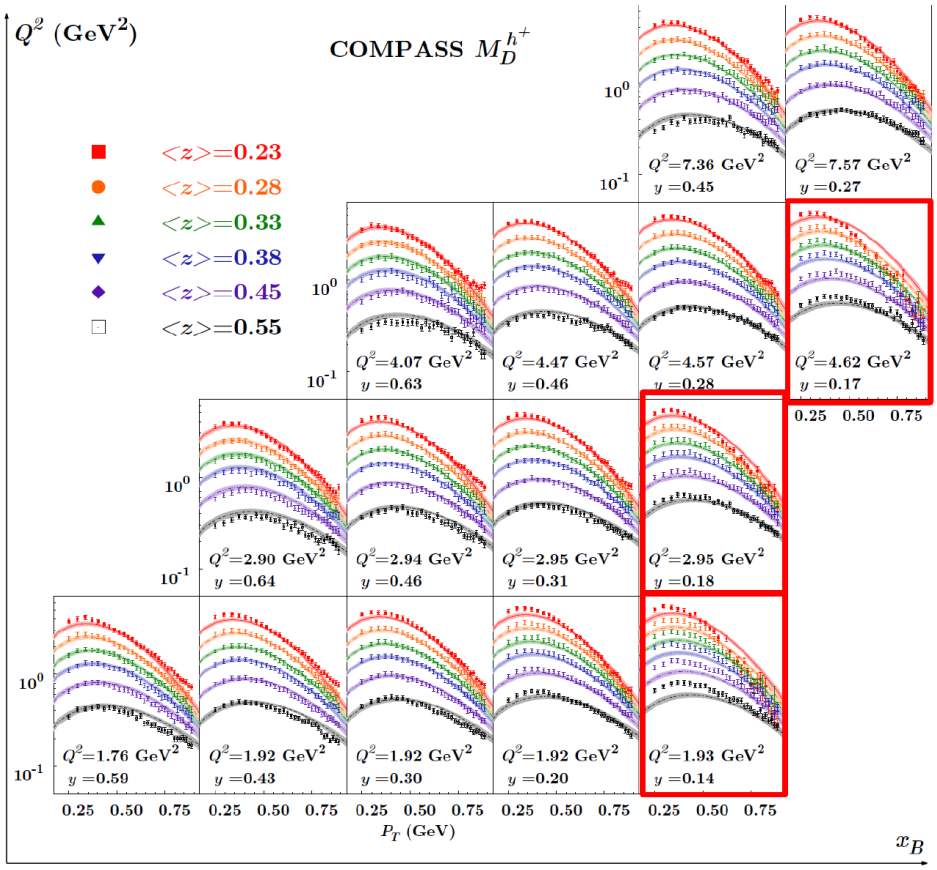

Figure 2. The multiplicities obtained including the y-dependent normalisation factor of Eq. (7) are compared with the COMPASS measurements for h^+ SIDIS production off a deuteron target. The shaded uncertainty bands correspond to a 5% variation of the total χ^2. It is interesting to note that about 50% of the value of χ^2 comes from the three panels inside red boxes, which enclose the bins with lowest value of y.

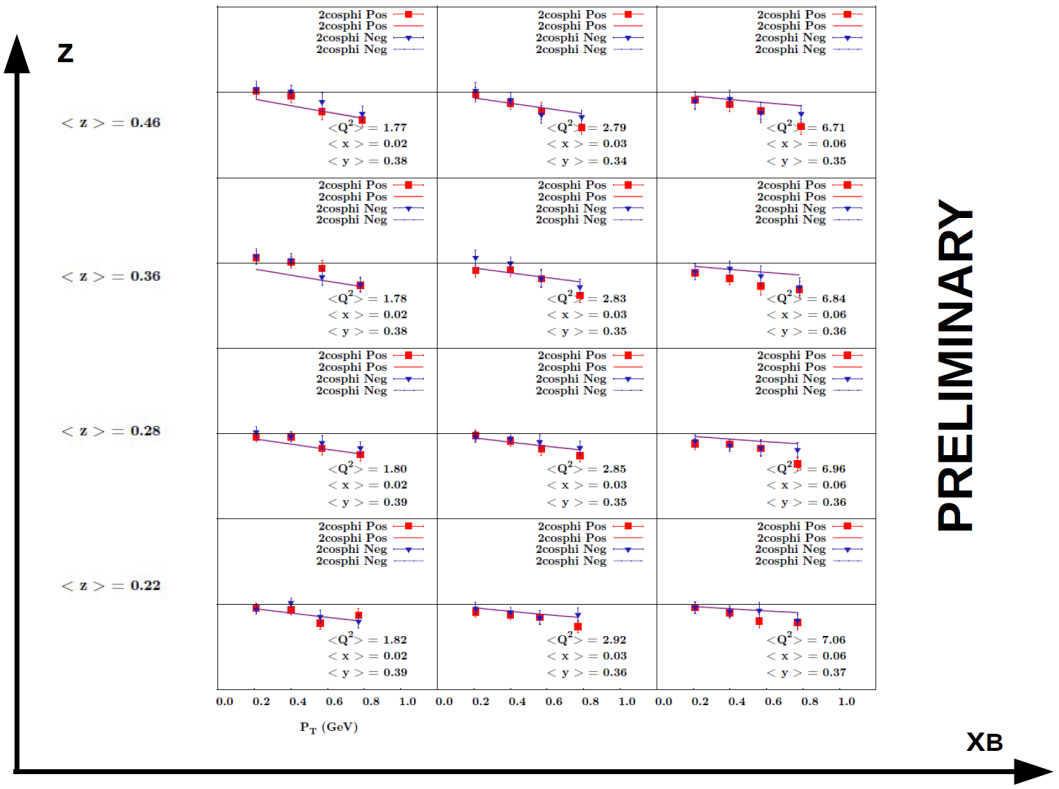

Figure 3. Comparson of $\langle cos(\phi) \rangle$ data with minimal curves, obtained from a simultaneous fit of COMPASS multiplicities and $\langle cos(\phi) \rangle$. For this preliminary fit, Eqs. (2-6) and Eq. (10) were used. The kinematical cuts are those shown in Table 1.